Drag diagrams computed by an integral method are shown in Fig. 3 for a permeable plate whose boundary layer is turbulized for $r = 10^6$. It is seen that as the concentration c_w of the delivered solution increases in each boundary layer section, the effect of reducing the friction first grows and then when the quantity c_e exceeds the optimal macromolecule concentration, starts to be reduced. The joint influence of injection and polymer admixtures permits obtaining a substantial reduction in turbulent friction even for very large values of v_w/u_δ.

Notation. u_δ is the free stream velocity; u_τ is the dynamic velocity; τ_w is the tangential stress on the wall; q_w is the diffusion impurity flux through the permeable wall; ν and ν_t are molecular and turbulent viscosity coefficients; c_w is the impurity concentration on the wall; δ and δ_v are boundary layer and viscous sublayer thicknesses; Sc and Sc_t are the molecular and turbulent Schmidt numbers; z and y are the longitudinal and transverse coordinates and c_f is the local friction drag coefficient.

LITERATURE CITED

1. V. A Ioselevich, Vestn., Mosk. Gos. Univ., Mat. Mekh., No. 6, 38-42 (1986).
2. S. S. Kutateladze, Principles of Heat Transfer Theory [in Russian], Moscow (1979).
3. V. A. Ioselevich, Mechanics and Scientific-Technical Progress [in Russian], 2, 146-163 (1987).
4. V. M. Eroshenko and L. I. Zaichik. Hydrodynamics and Heat Transfer on Permeable Surfaces [in Russian], Moscow (1984).

MATHEMATICAL MODELLING OF NONISOTHERMAL TURBULENT ONE- AND TWO-PHASE SWIRLING FLOWS

V. V. Novomlinskii

UDC 532.529

A mathematical model is developed and realized numerically for turbulent gas-dispersed nonisothermal swirling flows on the basis of Navier—Stokes type equations by using a modified k—ε turbulence model. Corrections taking account of the influence of particles and the flow swirling on k, ε are introduced into these latter. A finite-difference method of controlled volume is used to solve the equations. Computations are compared with experimental data on swirling single-phase flows in a cylindrical channel. Data are obtained about the influence of the nonisothermy on the length of the recirculation zone.

Introduction. Two-phase (gas—solid or liquid particles) turbulent high-temperature swirling flows are utilized extensively in plasma technology, plasma chemistry, and powder metallurgy. The investigation of such flows and the subsequent development of existing technologies on this basis can be carried out, in particular, by constructing numerical models of these processes and executing numerical experiments by using such models, as would permit determination of the most important flow characteristics, the velocity, phase temperatures, powder concentration, etc.

Different turbulent two-phase jet flows, computation methods, and results of numerical modelling are presented in [1]. The extensively known Prandtl mixing-path model modified by G. N. Abramovich for gas-dispersed flows, is used as the closure model.

Turbulent swirling flows are utilized for intensification of heat and mass transfer processes in different apparatus as well as for electric arc stabilization in plasmatrons. It is known that strongly swirling flows are characterized by the occurrence of recirculation

Ordzhonikidze Moscow Aviation Institute. Translated from Inzhenerno-fizicheskii Zhurnal, Vol. 60, No. 2, pp. 191-197, February, 1991. Original article submitted December 9, 1989.

 0022-0841/91/6002-0148$12.50

zones in the form of near-axis toroidal vortices. Various factors, in particular, the configuration of the flow domain boundaries, the degree of nonisothermy, the intenseness of the initial swirling, as well as the degree of flow charging by particles in the case of gas-dispersed flows affect the location and size of these zones.

Results of a theoretical and experimental investigation of weakly and strongly swirling flows by using different turbulence models are presented in [1].

Formulation, Method of Solution, and Results of Computations. The hypothesis of interpenetrating, interacting continuums is used in this paper to model two-phase flows. Turbulent subsonic gas flows with particles of 20-60 μm size whose bulk concentration is $\gamma \sim 10^{-3}$ are examined. It is shown in [1] that for $\gamma < 2 \cdot 10^{-2}$ particle interaction with each other can be neglected. Phase dispersion is simulated by a set of solid or liquid spheres of identical dimensions, where the intrinsic particle volume is not taken into account. The density of the dispersed phase $\Theta = \rho_p \gamma$ is comparable to the density ρ of the carrying gas. For inert particles ($\rho/\rho_p \ll 1$) all the forces acting on a single particle, except the drag force, are ordinarily neglected. The two-phase flow is assumed substantially nonequilibrium. The particle turbulent diffusion process can be neglected for two-phase flows with inert particles and small time, this is given a foundation in detail in [2]. Known empirical relationships taking account of the inertia and rarefaction of the flow as well as the high temperature drops on the gas-particle boundary [3, 4] are used for the drag and heat transfer coefficients of a single particle. Particle heating is assumed gradient-free and radiant heat transfer is neglected.

Turbulence is described by using a two-parameter k–ε closure model. Applying the Friedman–Keller procedure, additional source terms can be obtained in the k and ε-equations that reflect the influence of the dispersed phase on the fluctuation energy k and the specific velocity of dissipation of the fluctuation energy ε [5]. It was assumed in the derivation of these terms that the dispersed phase can be considered as a continuous medium in the L_k scales, for large-scale energy carrying vortices, and in the L_ε scales for fine-scale dissipative vortices. The mean distance between particles is $L_c \sim \gamma^{-1/3} d_p$ and much greater than $L_\varepsilon \sim L_0 Re^{-3/4}$ in many practical cases and much less than $L_k \sim L_0$, where L_0 is the characteristic dimension of the flow domain and d_p is the particle diameter. This makes formal application of the Friedman–Keller procedure impossible for obtaining the source term $S_{\varepsilon p}$. In the case $L_c \gg L_\varepsilon$ and $\gamma \ll 1$ an additional source term for the ε-equation of $S_{\varepsilon p}$ can be neglected [2].

It is known that the influence of flow swirling on the fluctuation characteristics is complete in nature. Cases of both turbulent fluctuation generation and suppression are possible under the action of flow rotation. The stability criterion of swirling flows to random perturbations was examined in [6]

$$\frac{\partial (w^2/r)}{\partial r} \geqslant 0.$$

It is asserted that upon compliance with this condition swirling suppresses turbulent velocity fluctuations and the intensity of turbulence diminishes.

No sufficiently adequate reality exists at this time for the turbulence model for swirling flows. A new modification of the k–ε turbulence model is proposed in this paper for the case of swirling flows that takes account of both turbulence and suppression of turbulence under the influence of swirling and going over to a standard k–ε model upon damping of the swirling. The kind of component characterizing generation in the ε-equations is changed. The turbulent viscosity μ_t increases for additional turbulization under the action of swirling and μ_t diminishes under the suppression of the turbulent velocity fluctuations. A change in μ_t can be obtained by modifying the expression for c_1. The generation term G equals the sum of G_w and $G_{u,v}$, where G_w is the generation due to the tangential velocity component w with strengthened influence of the moment, which is conformity with the gradient hypothesis can be represented as

$$\langle F_r' v' \rangle = -\mu_t \frac{\partial (w^2/r)}{\partial r},$$

where F_r' is the fluctuating component of the centrifugal force. The term $G_{u,v}$ is generation due to the u,v velocity components:

$$G_w = \mu_t\left[\left(r\frac{\partial}{\partial r}\left(\frac{w}{r}\right)\right)^2 + \left(\frac{\partial w}{\partial z}\right)^2 - \frac{\partial (w^2/r)}{\partial r}\right];$$

$$G_{u,v} = 2\mu_t\left[\left(\frac{\partial u}{\partial z}\right)^2 + \left(\frac{\partial v}{\partial r}\right)^2 + \left(\frac{v}{r}\right)^2\right] + \mu_t\left(\frac{\partial u}{\partial r} + \frac{\partial v}{\partial z}\right)^2.$$

The increase (diminution) in μ_t is achieved by diminution (increase) of the component $c_1G\varepsilon/k$ in the equation for ε. Using a simple analog for the Richardson number Ri in the form $Ri = G_w/(G_{u,v} + G_w)$ the quantity c_1 can be given as:

$$c_1 = 1{,}44 - c_3\,\mathrm{Ri}.$$

Therefore, depending on the sign of the number Re the coefficient c_1 increases in the case of flows with turbulence suppression and diminishes for flows with turbulence intensification. The best correspondence with experimental data is obtained for $c_3 \approx 1$, i.e., $c_1 = 1.44 - \mathrm{Ri}$. Comparing the computations by using the proposed model with other computations and experiments showed that the model with the correction for c_1 describes the flow characteristics sufficiently exactly [2].

Nonisothermal swirling one- and two-phase flows were investigated in this research. Equations of the type of the complete Navier–Stokes energy and continuity equations for averaged parameters in a cylindrical coordinate system under axial symmetry conditions were written for the gas phase. The gas density and particle parameter fluctuations were neglected in writing these equations:

$$\frac{\partial \rho u r}{\partial z} + \frac{\partial \rho v r}{\partial r} = 0;$$

$$\rho u\frac{\partial u}{\partial z} + \rho v\frac{\partial u}{\partial r} = -\frac{\partial P}{\partial z} + \frac{\mu_s}{3}\frac{\partial}{\partial z}\,\mathrm{div}\,\mathbf{V} + \mu_s\Delta u -$$

$$-\frac{2}{3}\,\mathrm{div}\,\mathbf{V}\frac{\partial \mu_s}{\partial z} + 2\varepsilon_{rz}\frac{\partial \mu_s}{\partial r} + 2\varepsilon_{zz}\frac{\partial \mu_s}{\partial z} - \frac{2}{3}\frac{\partial}{\partial z}(\rho k) + S_{up};$$

$$\rho u\frac{\partial v}{\partial z} + \rho v\frac{\partial v}{\partial r} - \frac{\rho w^2}{r} = -\frac{\partial P}{\partial r} + \frac{\mu_s}{3}\frac{\partial}{\partial r}\,\mathrm{div}\,\mathbf{V} +$$

$$+\mu_s\left(\Delta v - \frac{v}{r^2}\right) - \frac{2}{3}\frac{\partial \mu_s}{\partial r}\,\mathrm{div}\,\mathbf{V} + 2\varepsilon_{rr}\frac{\partial \mu_s}{\partial r} +$$

$$+ 2\varepsilon_{rz}\frac{\partial \mu_s}{\partial z} - \frac{2}{3}\frac{\partial}{\partial r}(\rho k) + S_{vp};$$

$$\rho u\frac{\partial w}{\partial z} + \rho v\frac{\partial w}{\partial r} + \frac{\rho v w}{r} = \mu_s\left(\Delta w - \frac{w}{r^2}\right) +$$

$$+ 2\varepsilon_{r\varphi}\frac{\partial \mu_s}{\partial r} + 2\varepsilon_{\varphi z}\frac{\partial \mu_s}{\partial z} + S_{wp};$$

$$\rho u\frac{\partial h}{\partial z} + \rho v\frac{\partial h}{\partial r} = \mathbf{V}\nabla P + \frac{1}{r}\frac{\partial}{\partial r}\left[r\left(\frac{\mu_t}{Pr_t} + \frac{\mu}{Pr}\right)\frac{\partial h}{\partial r}\right] +$$

$$+ \frac{\partial}{\partial z}\left[\left(\frac{\mu_t}{Pr_t} + \frac{\mu}{Pr}\right)\frac{\partial h}{\partial z}\right] + S_{hp}.$$

The equations of the two-parameter model of turbulence appear as follows:

$$\rho u\frac{\partial k}{\partial z} + \rho v\frac{\partial k}{\partial r} = \frac{1}{r}\frac{\partial}{\partial r}\left[\left(\frac{\mu_t}{\sigma_k} + \mu\right)\frac{\partial k}{\partial r}\right] +$$

$$+\frac{\partial}{\partial z}\left[\left(\frac{\mu_t}{\sigma_k}+\mu\right)\frac{\partial k}{\partial z}\right]+G-\rho\varepsilon+S_{kp};$$

$$\rho u\frac{\partial \varepsilon}{\partial z}+\rho v\frac{\partial \varepsilon}{\partial r}=\frac{1}{r}\frac{\partial}{\partial r}\left[\left(\frac{\mu_t}{\sigma_\varepsilon}+\mu\right)\frac{\partial \varepsilon}{\partial r}\right]+$$

$$+\frac{\partial}{\partial z}\left[\left(\frac{\mu_t}{\sigma_\varepsilon}+\mu\right)\frac{\partial \varepsilon}{\partial z}\right]+c_1\frac{\varepsilon}{k}G-c_2\rho\frac{\varepsilon^2}{k},$$

where

$$\rho=\rho(T);\quad \mu=\mu(T);\quad \varepsilon_{rz}=\frac{1}{2}\left(\frac{\partial v}{\partial z}+\frac{\partial u}{\partial r}\right);$$

$$\varepsilon_{rr}=\frac{\partial v}{\partial r};\quad \varepsilon_{\varphi z}=\frac{\partial w}{\partial z};\quad \varepsilon_{zz}=\frac{\partial u}{\partial z};\quad \varepsilon_{\varphi r}=\frac{1}{2}\left(\frac{\partial w}{\partial r}-\frac{w}{r}\right);$$

$$\mathbf{V}=(u,\ v,\ w);\quad \operatorname{div}\mathbf{V}=\frac{\partial u}{\partial z}+\frac{1}{r}\frac{\partial}{\partial r}(rv);\quad \mu_s=\mu_t+\mu;$$

$$\mu_t=c_\mu\rho k^2/\varepsilon;\quad \Delta v=\frac{1}{r}\frac{\partial}{\partial r}\left(r\frac{\partial v}{\partial r}\right)+\frac{\partial^2 v}{\partial z^2};$$

$$c_1=1{,}44-\mathrm{Ri};\quad \mathrm{Ri}=G_w/G;\quad G=G_{u,v}+G_w.$$

For additional source terms reflecting the influence of particles on the gas, we write the relationships

$$S_{up}=\Theta(u_p-u)/\tau_D;\quad S_{vp}=\Theta(v_p-v)/\tau_D;\quad S_{wp}=\Theta(w_p-w)/\tau_D;$$

$$S_{hp}=\frac{\Theta}{\tau_T}\int_T^{T_p}\lambda dT;\quad \Theta=\gamma\rho_p;\quad S_{\kappa p}=-2k\Theta/\tau_D^*.$$

Euler type equations [2] are used for the dispersed phase [2]:

$$\frac{\partial\gamma u_p r}{\partial z}+\frac{\partial\gamma v_p r}{\partial r}=0;\quad v_p\frac{\partial v_p}{\partial r}+u_p\frac{\partial v_p}{\partial z}-\frac{w_p^2}{r}=-S_{vp}/\Theta;$$

$$u_p\frac{\partial u_p}{\partial z}+v_p\frac{\partial u_p}{\partial r}=-S_{up}/\Theta;\quad v_p\frac{\partial w_p}{\partial r}+u_p\frac{\partial w_p}{\partial z}+\frac{v_p w_p}{r}=-S_{wp}/\Theta;$$

$$u_p\frac{\partial h_p}{\partial z}+v_p\frac{\partial h_p}{\partial r}=-S_{hp}/\Theta.$$

Auxiliary relationships are written in the form [2-4]

$$\tau_D=\rho_p d_p^2/18\mu f_D;\quad f_D=\frac{1+0{,}15\,\mathrm{Re}_p^{2/3}}{1+3{,}82A};\quad A=\mu/\rho c d_p;$$

$$\tau_D^*=\tau_D\left(1-\mathrm{Re}_p\frac{\partial\ln\tau_D}{\partial\,\mathrm{Re}_p}\right)^{-1};\quad \tau_T=\rho_p d_p^2/6\,\mathrm{Nu}_p;$$

$$\mathrm{Nu}_p=\frac{\mathrm{Nu}_{p0}}{1+3{,}42A\,\mathrm{Nu}_{p0}/\mathrm{Pr}};\quad \mathrm{Nu}_{p0}=2\,(\lambda/\lambda(T_p))+$$

$$+0{,}6\,\mathrm{Re}_p^{0,5}\,\mathrm{Pr}^{0,33}\,(\rho\mu/\rho(T_p)\,\mu(T_p))^{0,2};\quad \mathrm{Re}_p=\rho d_p\,|u-u_p|/\mu.$$

Profiles obtained experimentally, or certain model profiles (for u, k, ε, h, γ, u_p, h_p homogenous, v, v_p equality to zero, w, w_p according to the law of rotation of a solid) were given at the entrance to the channel (nozzle exit). Symmetry conditions were given on the channel axis, and "soft" boundary conditions at the exit from the channel. Adhesion and isothermy conditions were realized on the wall while for k and ε a modification of the Lamb and Bramhorst k–ε model [7], proposed for near-wall flows, was selected.

A Patankar (SIMPLE-procedure) [8] finite-difference controlled volume method was used to solve the Navier–Stokes type equations. The scheme of "against the flow" and the more accurate "degree" [8] were used to approximate the convective terms. The difference equations obtained were solved by iteration and three-point factorization were used at each iteration. The so-called "checkerboard" mesh in which the values of u and v were determined at the half-nodes of the difference mesh was used to compute the flow field while the remaining quantities were determined at the integer nodes. The pressure was determined from the

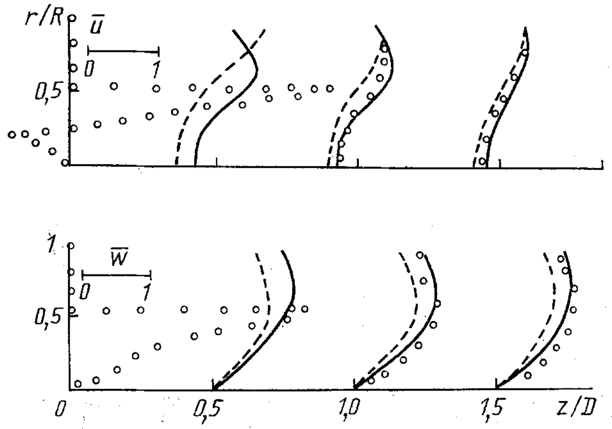

Fig. 1. Radial u, w profiles for strongly swirling single-phase flow in a pipe.

difference analog of the continuity equation. The method of solution is described in detail in [8].

Experimental data and computations for anisothermal swirling air flow in a pipe are presented in [9, 10]. The Reynolds number varied between $5.3 \cdot 10^4$ and $1.5 \cdot 10^5$ while the geometric angle of the swirling φ_H took on the values 0, 38, 45, 60 and 70°. Comparing the experimental and computed data shows that the model with the correction for c_1 more accurately predicts the averaged (u, w) and fluctuating (k, ε) parameters of strongly swirling flow in a channel.

Dimensionless radial u and w profiles are shown in Fig. 1 for $\varphi_H = 70°$, obtained experimentally and in computations using two models (points are experiment [9], dashed lines are the computation in [10] and solid lines are computation using the k–ε model with the correction for c_1).

The next part of the computation was performed to study propagation of a "hot" swirling air jet in a "cold" space. The purpose of the investigation is to determine the influence of the degree of nonisothermy α of the flow (where $\alpha = T_c/T_\infty$, T_c is the initial jet temperature, and $T_\infty = 300$ K is the temperature of surrounding space) and the initial swirling level w_0 on the size of the recirculation zone that occurs in a strongly swirling jet (Fig. 2). In the case of the outflow of a "hot" jet (α = 2; 3.3) the length of the recirculation zone diminishes substantially, where the critical value of w_0 for which a reverse flow is formed increases.

The swirling turbulent air flow with nickel particles ($d_p = 20$ μm) in a cylindrical channel was also investigated numerically. The ratio between the particle and gas mass flow rates was one. The presence of an inert phase in the swirling flow resulted in growth of the impurity concentration at the channel wall, diminution of the recirculation zone length in strongly swirling flows, deformation of the radial profiles of all the parameters. The presence of an initially unswirling disperse phase suppresses the recirculation zone, as the computations showed. Radial u, u_p profiles are shown in Fig. 3 for a strongly swirling flow in a pipe [curves 1) gas velocity u for two-phase flow; 2) u_p in this same case; 3) gas velocity for a single-phase swirling flow].

Conclusion. The model developed for two-phase turbulent nonisothermal flows with particles several tens of microns in size permits determination of the flow parameters during plasma technology processes. The model is approved according to known experimental data. Results are presented on the influence of swirling intensity and degree of nonisothermy on the size of the recirculation zone.

Notation. k is the kinetic energy of turbulent pulsations; ε is the specific rate of dissipation of fluctuation energy; γ is bulk particle concentration; Θ is disperse phase density; ρ_p is density of particle substance; ρ is gas density; L_k, L_ε are scales of energy carrying and dissipative turbulence vortices, respectively; L_c is the mean distance between particles; L_0 is the characteristic dimension of the flow domain; d_p is the particle diameter; Re, Pr are the Reynolds and Prandtl numbers; S_{up}, S_{vp}, S_{wp}, S_{kp}, $S_{\varepsilon p}$, S_{hp} are additional

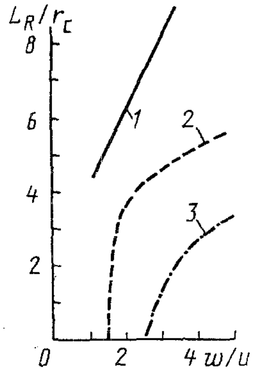

Fig. 2

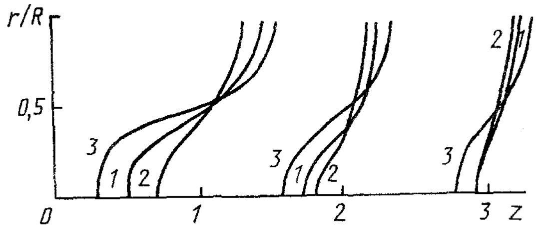

Fig. 3

Fig. 2. Dependence of the recirculation zone length L_R on the initial swirling level w_0 and the degree of nonisothermy α: 1) $\alpha = 1$; 2) 2; 3) 3.3.

Fig. 3. Radial u, u_p profiles for strongly swirling two-phase flow in a pipe.

source terms reflecting the influence of the disperse phase; u, v, w—z, r, φ are average gas velocity components in a cylindrical coordinate system; G, $G_{u,v}$, G_w is the generation term in the turbulence model and its components; c_μ, c_1, c_2, σ_k, σ_ε are empirical quantities of the k—ε model; Ri is the Richardson number; μ_t, μ, μ_s are turbulent, laminar, and effective viscosities; ρ, λ, P is the gas density, heat conductivity, and pressure; h is the gas enthalpy; Pr_t is the turbulent Prandtl number; u_p, v_p, w_p, h_p are velocity and enthalpy components of the disperse phase; T, T_p are the gas and particle temperatures; τ_D, τ_T are the dynamic relaxation time and the coefficient of thermal particle relaxation in the flow; f_D is the correction to the particle flow mode instability; c is the speed of sound; Re_p, Nu_p are the Reynolds and Nusselt numbers for particles; φ_H is the geometric angle of swirl; α is the degree of flow nonisothermy; and L_R is the recirculation zone length.

LITERATURE CITED

1. J. Schatz, Turbulent Flow. Injection and Mixing Processes [Russian translation], Moscow (1984).
2. V. V. Novomlinskii and M. P. Strongin, Prikl. Mekh. Tekh. Fiz., No. 2, 51-58 (1988).
3. D. Carlson and R. Hoaglund, AIAA Jnl. [Russian translation], No. 1, 104-109 (1964).
4. I. S. Burov, Fiz. Khim. Obrap. Mat., No. 4, 42-49 (1979).
5. S. A. Kantor, M. P. Strongin, and I. Ya. Yatskar', "Turbulent two-phase flows," Abstract of Reports, Fourth All-Union Sci. Conf., 88-92 [in Russian], Tallin (1982).
6. G. E. Sturov, Izv. Sib. Otd. Akad. Nauk SSSR, Ser. Tekh. Nauk, Issue 3, No. 16, 32-33 (1984).
7. G. Lamb and K. Ramhorst, Tr. Am. O-va Inzh.-Mekh. Teor. Osn. Inzh., 103, No. 3, 156-160 (1981).
8. S. Patankar, Numerical Methods of Solving Fluid Heat Transfer and Dynamics Problems [in Russian], Moscow (1984).
9. H. K. Yoon and D. G. Lilley, AIAA Paper No. 315 (1983).
10. M. T. Abujelala and D. G. Lilley, AIAA Paper No. 441 (1984).